

QUANTUM PARAELECTRICITY AND INDUCED FERROELECTRICITY BY GERMANIUM DOPING OF $(\text{Pb}_y\text{Sn}_{1-y})_2\text{P}_2\text{S}(\text{Se})_6$ SINGLE CRYSTALS

I. Zamaraitė^a, A. Džiaugys^a, Yu. Vysochanskii^b, and J. Banys^a

^aFaculty of Physics, Vilnius University, Saulėtekio 9, 10222 Vilnius, Lithuania

^bInstitute of Solid State Physics and Chemistry, Uzhgorod University, 46 Pidgirna St., 88000 Uzhgorod, Ukraine

Email: ilona.zamaraitė@ff.vu.lt

Received 24 January 2020; revised 26 March 2020; accepted 6 April 2020

In this paper we report a dielectric study on four single crystals $\text{Pb}_2\text{P}_2\text{S}_6$, $(\text{Pb}_{0.98}\text{Ge}_{0.02})_2\text{P}_2\text{S}_6$, $(\text{Pb}_{0.7}\text{Sn}_{0.3})_2\text{P}_2\text{S}_6 + 5\% \text{Ge}$ and $(\text{Pb}_{0.7}\text{Sn}_{0.3})_2\text{P}_2\text{Se}_6 + 5\% \text{Ge}$ down to 20 K. A new quantum paraelectric state was reported in the Ge-doped samples at low temperatures. In all of these materials the non-classical T^2 temperature dependences of inverse dielectric permittivity were observed. The dielectric constants of $\text{Pb}_2\text{P}_2\text{S}_6$ -based single crystals were measured between 20 and 300 K. The temperature dependences of dielectric permittivity were analysed on the basis of Barrett's model as a signature of quantum paraelectricity.

Keywords: dielectric properties, ferroelectric phase transition, quantum paraelectricity, phosphorus chalcogenide crystals, $\text{Pb}_2\text{P}_2\text{S}_6$

PACS: 77.22.-d, 77.80.B-

1. Introduction

For $\text{Sn}_2\text{P}_2\text{S}_6$ (SPS) ferroelectrics the second-order phase transition at $T_0 \sim 337$ K with a mixed displacive–order/disorder character occurred [1]. SPS is the most prominent example of ferroelectric ternary phosphorus chalcogenide crystals represented by the general formula $M_2\text{P}_2\text{X}_6$ (where M is transition or post-transition carbon group p metals, X is chalcogenides). Moreover, optical measurements have proven $\text{Sn}_2\text{P}_2\text{S}_6$ as a semiconductor with a relatively narrow bandgap and promising photorefractive, photovoltaic, electrooptic and piezoelectric features [2, 3]. Another feature, that makes them very attractive for the researchers, is an isovalent anion substitution into the crystal lattice producing series of $(\text{Pb}_y\text{Sn}_{1-y})_2\text{P}_2(\text{Se}_x\text{S}_{1-x})_6$ mixed crystals. The impact of dopants on the ferroelectricity of crystals has a special attention as

an effective engineering approach that introduces changes into the position or character of the phase transition and physical properties.

$\text{Sn}_2\text{P}_2\text{S}_6$ crystal is a uniaxial proper ferroelectric with a three-well local potential for order parameter fluctuations [4, 5]. The ferroelectric phase transition of $\text{Sn}_2\text{P}_2\text{S}_6$ is induced by stereoactivity of the Sn^{2+} cation $5s^2$ electron lone pair: antibonding mixing of tin and sulfur orbitals ($5s$ and $3p$, respectively) interacts with the tin $5p$ orbitals, generating lower energy filled states $\text{Sn } 5\nu$ ($\text{Sn } 5s + \text{S } 3p$). This formation of the Sn^{2+} lone pair electron cloud, together with the deformation of the nearest polyhedron formed by sulfur atoms, determines the origin of spontaneous polarization [4, 6].

The experimental results of $(\text{Pb}_y\text{Sn}_{1-y})_2\text{P}_2\text{S}_6$ showed that the phase diagram of $(\text{Pb}_y\text{Sn}_{1-y})_2\text{P}_2\text{S}_6$ could be quite complicated with possible coexistence of ferroelectric-paraelectric states [7, 8]. This is

in agreement with the thermodynamical description based on the Blume–Emery–Griffith (BEG) model with random bond and random field defects, where the introduction of Pb is responsible for the randomness [9]. One more feature of the phase diagram predicted by the BEG model is the presence of tricritical point (TCP). According to the experimental data, for the $(\text{Pb}_y\text{Sn}_{1-y})_2\text{P}_2\text{S}_6$ mixed crystals the paraelectric phase becomes stable above $y > 0.7$ at a normal pressure [10, 11]. Also, in previous papers it was shown that for $y > 0.3$ and below 220 K the hysteresis appears [8]. It was related to the coexistence of paraelectric and ferroelectric phases, and evidenced a discontinuous character of the phase transition [9]. The phase diagram of these mixed crystals with substitution of tin for lead or sulfur for selenium is really an interesting point that was investigated in-depth in several studies [1, 7–8, 12–13].

SrTiO_3 in a chemically pure form was reported as a typical quantum paraelectric featured by high dielectric permittivity ϵ and low dielectric loss $\tan\delta$, absent from ferroelectric transitions down to the lowest temperatures [14, 15]. This effect is attributed to large quantum fluctuations in the limit of absolute zero temperature [15]. SrTiO_3 , CaTiO_3 and KTaO_3 are also classified as quantum paraelectrics or incipient ferroelectrics which possess a high dielectric constant [16]. Very similar effects are also observed in the chemically or isotopic substituted SrTiO_3 ($\text{SrTiO}_3:\text{Ca}$ or $\text{SrTiO}_3:\text{O}^{18}$) [17].

A key factor in the pure $\text{Pb}_2\text{P}_2\text{S}_6$ single crystal is ‘quantum paraelectric state’ [8], as it was classified according to the study of Müller et al. [14]. The phase diagram of $(\text{Pb}_y\text{Sn}_{1-y})_2\text{P}_2\text{S}_6$ mixed crystals was examined systematically. Quite often, the material can be tuned to a quantum critical point (QCP) by applying pressure or changing the chemical composition in mixed crystals [18]. QCP is a point at absolute zero temperature in a phase diagram, where the quantum fluctuations drive a phase transition. Thus, it may seem that the quantum phase transition is an abstract theoretical idea. However, the influence of the critical point extends over a wide range at $T > 0$: this is the regime of quantum criticality.

We present in this paper the results of dielectric spectroscopic studies carried out on undoped $\text{Pb}_2\text{P}_2\text{S}_6$ and Ge-doped lead-based crystals that revealed the presence of quantum paraelectricity and induced ferroelectricity.

2. Results and discussion

In Fig. 1, the results of the dielectric permittivity of $\text{Pb}_2\text{P}_2\text{S}_6$ single crystal are presented. It is shown that for the $\text{Pb}_2\text{P}_2\text{S}_6$ single crystal, the real part of dielectric permittivity increases monotonously with decreasing temperature in the measured temperature range. The saturation behaviour of the real part of dielectric permittivity is not observed. The dispersion of the real part of dielectric permittivity was not detected. In the quantum critical regime the usual Curie–Weiss law of inverse dielectric permittivity $1/\epsilon(T) \sim T$ changes into $1/\epsilon(T) \sim T^2$ [18]. That is the most prominent criterion of quantum critical behaviour. Other quantities such as the thermal expansion coefficient and soft-mode frequencies are expected to vary in an unconventional manner. As shown in the inset of Fig. 1, the inverse dielectric permittivity $1/\epsilon(T)$ exhibits the expected non-classical T^2 temperature dependence over the finite temperature range above approximately 50 K and below 250 K. Typically, there is no ferroelectric phase transition in quantum paraelectrics, but critical behaviour, manifested by the non-classical T^2 dependence, occurs [19].

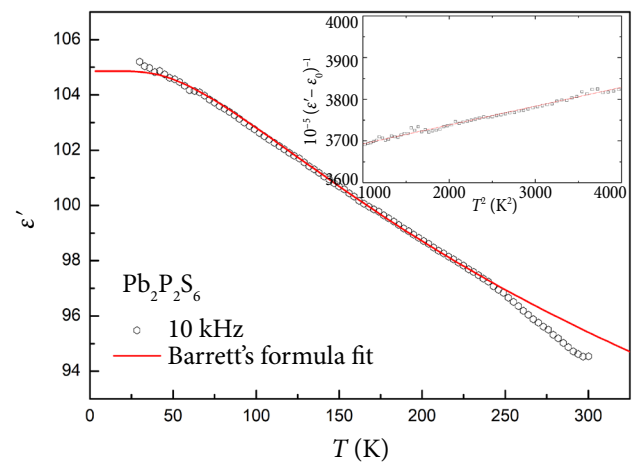


Fig. 1. Temperature dependences of the real part of dielectric permittivity of the $\text{Pb}_2\text{P}_2\text{S}_6$ single crystal. The inset shows the non-classical $1/\epsilon(T) \sim T^2$ behaviour of $\text{Pb}_2\text{P}_2\text{S}_6$ quantum paraelectric.

In order to describe the temperature dependences of the dielectric permittivity of quantum paraelectrics, Barrett extended the Slater’s mean-field theory by including the quantum effect, and an equation was derived as

$$\varepsilon(T) = \frac{C}{\frac{T_1}{2} \coth \frac{T_1}{2T} - \theta_{\text{CW}}} + \varepsilon_0, \quad (1)$$

where C is the Curie–Weiss constant, θ_{CW} can be recognized as the classical paraelectric Curie temperature, ε_0 is the temperature-independent constant, T is the sample temperature, and T_1 is recognized as the temperature at which the instability begins. Approximately, it may be said that T_1 is the dividing point between the low temperature where quantum effects are important so $\varepsilon(T)$ deviates from the Curie–Weiss law, and the high temperature region where a classical approximation and the Curie–Weiss law are valid [19].

In the low temperature region ($T < T_1$), the quantum effects are present. In many cases, $\theta_{\text{CW}} \leq 0$ K, which refers to the virtual transition temperature. Therefore, the material does not undergo a ferroelectric phase transition at any finite temperature because of the quantum effects. When θ_{CW} is finite and $\theta_{\text{CW}} < T_1$, the quantum fluctuations that occur below T_1 break the long-range ferroelectric order and stabilize the quantum paraelectric state in the sample, and a probable ferroelectric transition occurs at θ_{CW} [20]. The dielectric data of $\text{Pb}_2\text{P}_2\text{S}_6$, $(\text{Pb}_{0.98}\text{Ge}_{0.02})_2\text{P}_2\text{S}_6$, $(\text{Pb}_{0.7}\text{Sn}_{0.3})_2\text{P}_2\text{S}_6 + 5\%$ Ge and $(\text{Pb}_{0.7}\text{Sn}_{0.3})_2\text{P}_2\text{S}_6 + 5\%$ Ge single crystals were analysed on the basis of Barrett's formula (1). The results are presented in Figs. 1, 2, 4 and 5, respectively. The red (online) solid line is a data fitting with the Barrett's formula. The best-fit parameter values of all measured samples are summarized in Table 1.

The Barrett's formula has been reported as a fundamental model to describe the temperature behaviour of dielectric constant of the so-called incipient ferroelectrics (or quantum paraelectrics). However, discrepancies in the fitting with the Barrett's equation were reported by several authors. Then, various alternative models, in addition to the Barrett's model, have been proposed to explain the quantum

paraelectric state. Unfortunately, disagreements still exist in the results of analyses and interpretations based on different models. The authors in the [16] study analysed the temperature dependences of dielectric permittivity of the most-studied quantum paraelectrics SrTiO_3 and KTaO_3 on the basis of three different models (Barrett's model, Vendik model and quantum criticality) to determine the most appropriate standpoint. It was concluded that the dielectric permittivity at low temperatures cannot be described properly using the Barrett's formula. The Vendik model was more appropriate in the low-temperature approximation. So, at this time, minor deviations of the temperature dependences of quantum paraelectrics exist for different models and there is no single model appropriate in all temperature ranges. This way, the Barrett's model still remains as a starting point to determine quantum paraelectricity.

In the temperature dependences of the dielectric permittivity of $\text{Pb}_2\text{P}_2\text{S}_6$ single crystals the deviation from the Barrett's equation starts around 50 K. The abovementioned notes of applicability of various models are suitable to explain such discrepancy. The obtained parameter values ($T_1 = 190$ K and $\theta_{\text{CW}} = -376$ K) of pure single crystal $\text{Pb}_2\text{P}_2\text{S}_6$ demonstrate that the material does not undergo ferroelectric phase transition at any finite temperature.

Lead replaces tin and selenium takes the place of sulfur in the whole concentration range of $(\text{Pb}_y\text{Sn}_{1-y})_2\text{P}_2(\text{Se}_x\text{S}_{1-x})_6$ mixed crystals. In addition, these crystals can be doped with germanium Ge, antimony Sb or tellurium Te, but only in small percentages. Germanium is the most important dopant because it takes the place of tin in the $\text{Sn}_2\text{P}_2\text{S}_6$ -type crystals. It is known that tin ions play an important role in the ferroelectricity of the material. Introducing Ge atoms into the cation sublattice of SPS crystal enhances the stereoactivity of the cation sublattice, increasing the critical temperature and sharpening the phase

Table 1. Comparison of the values obtained by fitting the Barrett's relation (1) for various compounds.

Compound	C (K)	T_1 (K)	θ_{CW} (K)	ε_0
$\text{Pb}_2\text{P}_2\text{S}_6$	14000	190	-376	75
$(\text{Pb}_{0.98}\text{Ge}_{0.02})_2\text{P}_2\text{S}_6$	1208	207	39.9	35
$(\text{Pb}_{0.7}\text{Sn}_{0.3})_2\text{P}_2\text{S}_6 + 5\%$ Ge	30667	69.8	-4.1	86
$(\text{Pb}_{0.7}\text{Sn}_{0.3})_2\text{P}_2\text{S}_6 + 5\%$ Ge	34256	55.3	-5.7	370

transition character. An increase of the transition temperature has already been observed in the paper [21] measuring the temperature evolution of piezoelectric and pyroelectric coefficients. It is worth noting that when Pb substitutes for Sn, the hybridization becomes weaker, reducing the phase transition temperature. On the other hand, the Ge dopant in $\text{Pb}_2\text{P}_2\text{S}_6$ -type crystals plays an opposite role: it enhances the total stereoactivity of metallic cations in the crystal.

It is known that a small amount of impurities in quantum paraelectrics could induce ferroelectricity [22, 23]. The transition to a polar state appears above some impurity critical concentration x . A widely accepted viewpoint is that the ferroelectricity in doped quantum paraelectrics is determined by an off-centre position of impurity ions which produces electric dipoles that induce polarization [22]. So, it is interesting to investigate how germanium impurities can affect the quantum paraelectric state of $\text{Pb}_2\text{P}_2\text{S}_6$. Figure 2 shows the temperature dependence of the real part of $(\text{Pb}_{0.98}\text{Ge}_{0.02})_2\text{P}_2\text{S}_6$ dielectric permittivity. The inset of Fig. 2 confirms the non-classical T^2 behaviour of inverse dielectric permittivity. It is needless to say that T^2 temperature dependence is not valid at low temperatures. For the doped system $(\text{Pb}_{0.98}\text{Ge}_{0.02})_2\text{P}_2\text{S}_6$, both temperatures (T_1 and θ_{CW}) are finite (Table 1). Also, since $\theta_{\text{CW}} < T_1$ for $(\text{Pb}_{0.98}\text{Ge}_{0.02})_2\text{P}_2\text{S}_6$, it could be concluded that

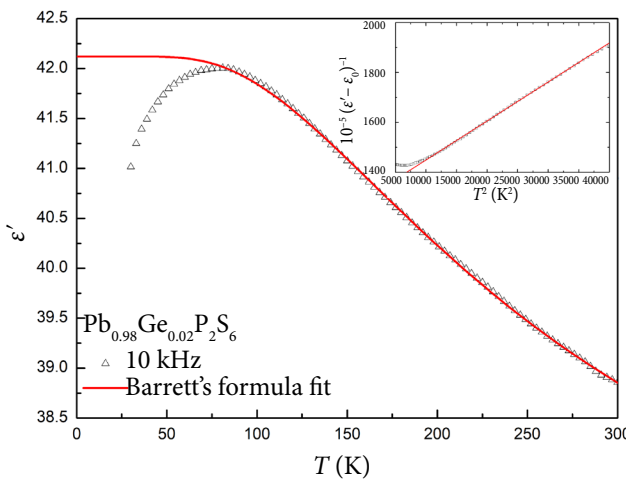


Fig. 2. Temperature dependence of the real part of complex dielectric permittivity of the $(\text{Pb}_{0.98}\text{Ge}_{0.02})_2\text{P}_2\text{S}_6$ single crystal sample. The inset shows the temperature dependence of inverse dielectric function in $(\text{Pb}_{0.98}\text{Ge}_{0.02})_2\text{P}_2\text{S}_6$.

the long-range ferroelectric order in this Ge-doped sample is broken due to quantum fluctuations below 207 K, and a probable ferroelectric transition occurs as manifested by a peak at 40 K for dielectric permittivity in Fig. 3. These differences of the $\text{Pb}_2\text{P}_2\text{S}_6$ and $(\text{Pb}_{0.98}\text{Ge}_{0.02})_2\text{P}_2\text{S}_6$ crystals could be related with different ionic radii of Pb^{2+} ($r_{\text{Pb}} = 1.33 \text{ \AA}$) and Ge^{2+} ($r_{\text{Ge}} = 0.87 \text{ \AA}$). The smaller germanium ionic radius results in different hybridization with the sulfur ions. Thus, doping with more stereoactive germanium cations induces some disorder effects and decreases dielectric permittivity value, below 75 K deviating from the Barrett's fit (Fig. 2). It suggests that possible phase transition might occur in this region.

Temperature dependence of the dielectric permittivity of $(\text{Pb}_{0.98}\text{Ge}_{0.02})_2\text{P}_2\text{S}_6$ at different frequencies is presented in Fig. 3. The peak of dielectric

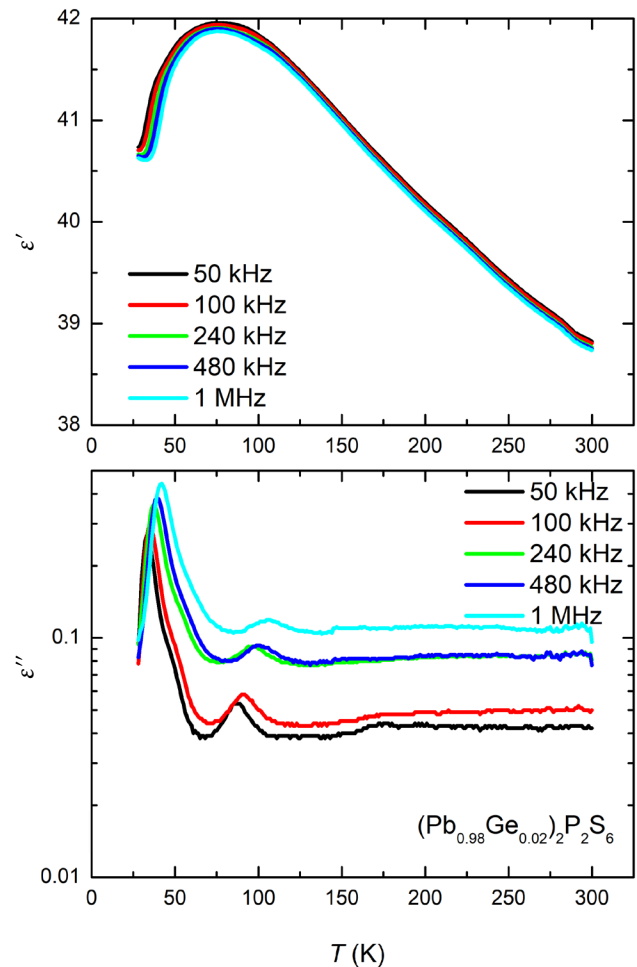


Fig. 3. Temperature dependence of the real and the imaginary parts of complex dielectric permittivity of the $(\text{Pb}_{0.98}\text{Ge}_{0.02})_2\text{P}_2\text{S}_6$ single crystal at selected frequencies.

permittivity is broad. The broadness of the phase transition is due to small compositional fluctuations. However, there are two peaks of the imaginary part of dielectric permittivity with a frequency dispersive behaviour, and the temperatures of loss peaks are around 50 and 100 K at 100 kHz.

The relaxation rate derived from the temperature dependence of the imaginary part of permittivity can be well fitted to the Arrhenius law

$$\nu = \nu_0 \exp\left(\frac{E_A}{kT}\right), \quad (2)$$

where ν_0 is the relaxation rate at the infinite temperature, E_A is the activation energy for the relaxation, k is the Boltzmann constant, and T is the temperature. The best-fitting value of activation energy is equal to 0.41 eV.

$\text{Pb}_2\text{P}_2\text{S}_6$ compound based mixed crystals have a stable paraelectric ground state till 0 K when lead concentration reaches $y \sim 0.7$ [8]. In previous papers it was shown that for $(\text{Pb}_y\text{Sn}_{1-y})_2\text{P}_2\text{S}_6$ mixed crystals with compositions $y \sim 0.61$ and $y \sim 0.65$ (which are close to the transition at zero temperature from the polar phase with $y < 0.7$ to the paraelectric one with $y > 0.7$) their dielectric susceptibility demonstrates the quantum critical behaviour in vicinity of the first-order transitions with $T_c \sim 35$ and 20 K, respectively [11]. To study the effect that the addition of Ge dopants has on the quantum paraelectric na-

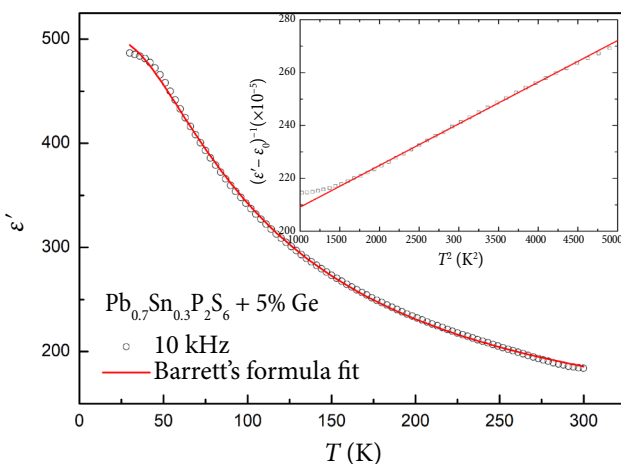


Fig. 4. Temperature dependence of the real part of complex dielectric permittivity of the $(\text{Pb}_{0.7}\text{Sn}_{0.3})_2\text{P}_2\text{S}_6 + 5\%$ Ge single crystal. Circles represent experimental data at 10 kHz, the solid curve shows fitting according to the Barrett's equation (1). The inset shows the temperature dependence of inverse dielectric function in $(\text{Pb}_{0.7}\text{Sn}_{0.3})_2\text{P}_2\text{S}_6 + 5\%$ Ge.

ture of $\text{Pb}_2\text{P}_2\text{S}_6$ compounds was precisely the aim of further investigations of $(\text{Pb}_{0.7}\text{Sn}_{0.3})_2\text{P}_2\text{S}_6 + 5\%$ Ge (Fig. 4) and $(\text{Pb}_{0.7}\text{Sn}_{0.3})_2\text{P}_2\text{Se}_6 + 5\%$ Ge (Fig. 5) samples. In these samples, Sn^{2+} sites codoping was realized by using two different ionic radius impurities – lead and germanium. It is worth reminding that the substitution for Sn has the strongest effect because the ferroelectric phase transition is induced by the stereoactivity of the Sn^{2+} cation $5s^2$ electron lone pair. However, it is known that lead and germanium have very different influences on the phase transitions.

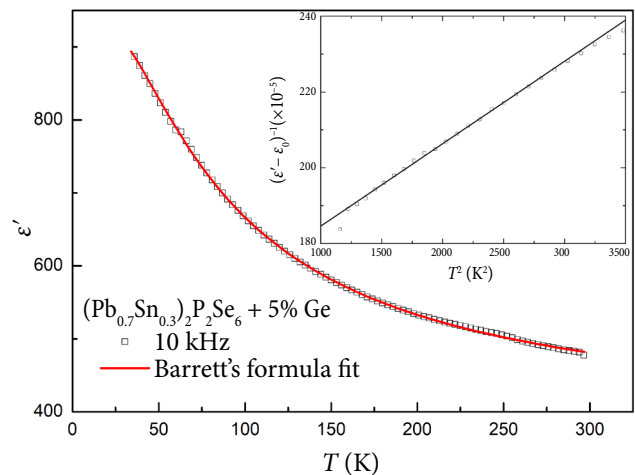


Fig. 5. Temperature dependence of the real part of complex dielectric permittivity of the $(\text{Pb}_{0.7}\text{Sn}_{0.3})_2\text{P}_2\text{Se}_6 + 5\%$ Ge single crystal. Squares represent experimental data at 10 kHz, the solid curve shows fitting according to the Barrett's equation (1). The inset shows the temperature dependence of inverse dielectric function in $(\text{Pb}_{0.7}\text{Sn}_{0.3})_2\text{P}_2\text{Se}_6 + 5\%$ Ge.

For $(\text{Pb}_{0.7}\text{Sn}_{0.3})_2\text{P}_2\text{S}_6 + 5\%$ Ge, by fitting to the Barrett's equation (1), $T_1 = 69.8$, $\theta_{\text{CW}} = -4.1$ and $C = 30677$ K were obtained. From Fig. 4 it can be seen that the fitting data are in good agreement with the experimental data. The obtained values demonstrate that the sample does not undergo a ferroelectric phase transition at any finite temperature.

3. Conclusions

We have carried out a dielectric study of four single crystals $\text{Pb}_2\text{P}_2\text{S}_6$, $(\text{Pb}_{0.98}\text{Ge}_{0.02})_2\text{P}_2\text{S}_6$, $(\text{Pb}_{0.7}\text{Sn}_{0.3})_2\text{P}_2\text{S}_6 + 5\%$ Ge and $(\text{Pb}_{0.7}\text{Sn}_{0.3})_2\text{P}_2\text{Se}_6 + 5\%$ Ge with a special emphasis on low temperatures. The temperature dependences of dielectric permittivity were

analysed in terms of the Barrett's model. This detailed analysis provided indications that $\text{Pb}_2\text{P}_2\text{S}_6$ -type crystals exhibit a quantum paraelectric state. By introducing small amounts (2%) of germanium dopants, the ferroelectric phase appears.

References

- [1] Y. Vysochanskii, T. Janssen, R. Currat, R. Folk, J. Banys, J. Grigas, and V. Samulionis, *Phase Transitions in Ferroelectric Phosphorous Chalcogenide Crystals* (Vilnius University Publishing House, Vilnius, 2008).
- [2] Y. Li and D.J. Singh, Properties of the ferroelectric visible light absorbing semiconductors: $\text{Sn}_2\text{P}_2\text{S}_6$ and $\text{Sn}_2\text{P}_2\text{Se}_6$, *Phys. Rev. Mater.* **1**(7), 075102 (2017), <https://doi.org/10.1103/PhysRevMaterials.1.075402>
- [3] M. Zhao, G. Gou, X. Ding, and J. Sun, Enhancing visible light absorption for ferroelectric $\text{Sn}_2\text{P}_2\text{S}_6$ by Se anion substitution, *J. Phys. Chem. C* **122**(44), 25565–25572 (2018), <https://doi.org/10.1021/acs.jpcc.8b08402>
- [4] K. Rushchanskii, Y. Vysochanskii, and D. Strauch, Ferroelectricity, nonlinear dynamics, and relaxation effects in monoclinic $\text{Sn}_2\text{P}_2\text{S}_6$, *Phys. Rev. Lett.* **99**(20), 207601 (2007), <https://doi.org/10.1103/PhysRevLett.99.207601>
- [5] R. Yevych, M. Medulych, and Y. Vysochanskii, Nonlinear dynamics of ferroelectrics with three-well local potential, *Condens. Matter Phys.* **21**(2), 23001 (2018), <https://doi.org/10.5488/CMP.21.23001>
- [6] K. Glukhov, K. Fedyo, J. Banys, and Y. Vysochanskii, Electronic structure and phase transition in ferroelectric $\text{Sn}_2\text{P}_2\text{S}_6$ crystal, *Int. J. Mol. Sci.* **13**(12), 14356–14384 (2012), <https://doi.org/10.3390/ijms131114356>
- [7] V. Shvalya, A. Oleaga, A. Salazar, A. Kohutych, and Y. Vysochanskii, Critical behaviour study of ferroelectric semiconductors $(\text{Pb}_x\text{Sn}_{1-x})_2\text{P}_2\text{S}_6$ from thermal diffusivity measurements, *Thermochim. Acta* **617**, 136–143 (2015), <https://doi.org/10.1016/J.TCA.2015.08.031>
- [8] R. Yevych, V. Haborets, M. Medulych, A. Molnar, A. Kohutych, A. Dziaugys, J. Banys, and Y. Vysochanskii, Valence fluctuations in $\text{Sn}(\text{Pb})_2\text{P}_2\text{S}_6$ ferroelectrics, *Low Temp. Phys.* **42**(12), 1155–1162 (2016), <https://doi.org/10.1063/1.4973005>
- [9] K. Ruzhchanskii, R. Bilanych, A. Molnar, R. Yevych, A. Kohutych, S. Perechinskii, V. Samulionis, J. Banys, and Y. Vysochanskii, Ferroelectricity in $(\text{Pb}_y\text{Sn}_{1-y})_2\text{P}_2\text{S}_6$ mixed crystals and random field BEG model, *Phys. Status Solidi B* **253**(2), 384–391 (2016), <https://doi.org/10.1002/pssb.201552138>
- [10] P. Ondrejko, M. Guennou, M. Kempa, Y. Vysochanskii, G. Garbarino, and J. Hlinka, An x-ray scattering study of $\text{Sn}_2\text{P}_2\text{S}_6$: Absence of incommensurate phase up to 1 GPa, *J. Phys. Condens. Matter* **25**(11), 115901 (2013), <https://doi.org/10.1088/0953-8984/25/11/115901>
- [11] K. Moriya, K. Iwachi, M. Ushida, A. Nakagawa, K. Watanabe, S. Yano, S. Motojima, and Y. Akagi, Dielectric studies of ferroelectric phase transitions in $\text{Pb}_{2x}\text{Sn}_{2(1-x)}\text{P}_2\text{S}_6$ single crystals, *J. Phys. Soc. Japan* **64**(5), 1775–1784 (1995), <https://doi.org/10.1143/JPSJ.64.1775>
- [12] A. Oleaga, V. Liubachko, A. Salazar, and Y. Vysochanskii, Introducing a tricritical point in $\text{Sn}_2\text{P}_2(\text{Se}_y\text{S}_{1-y})_6$ ferroelectrics by Pb addition, *Thermochim. Acta* **675**, 38–43 (2019), <https://doi.org/10.1016/J.TCA.2019.03.008>
- [13] V. Shvalya, A. Oleaga, A. Salazar, I. Stoika, and Y. Vysochanskii, Influence of dopants on the thermal properties and critical behavior of the ferroelectric transition in uniaxial ferroelectric $\text{Sn}_2\text{P}_2\text{S}_6$, *J. Mater. Sci.* **51**(17), 8156–8167 (2016), <https://doi.org/10.1007/s10853-016-0091-5>
- [14] K.A. Müller and H. Burkard, SrTiO_3 : An intrinsic quantum paraelectric below 4 K, *Phys. Rev. B* **19**(7), 3593–3602 (1979), <https://doi.org/10.1103/PhysRevB.19.3593>
- [15] T. Wei, C. Zhu, K.F. Wang, H.L. Cai, J.S. Zhu, and J.M. Liu, Influence of A-site codoping on ferroelectricity of quantum paraelectric SrTiO_3 , *J. Appl. Phys.* **103**(12), 124104 (2008), <https://doi.org/10.1063/1.2940372>
- [16] H. Fujishita, S. Kitazawa, M. Saito, R. Ishisaka, H. Okamoto, and T. Yamaguchi, Quantum paraelectric states in SrTiO_3 and KTaO_3 : Barrett model, Vendik model, and quantum criticality, *J. Phys. Soc. Japan* **85**(7), 074703 (2016), <https://doi.org/10.7566/JPSJ.85.074703>

- [17] C.W. Rischau, X. Lin, C.P. Grams, D. Finck, S. Harms, J. Engelmayer, T. Lorenz, J. Gallais, B. Fauqué, J. Hemberger, and K. Behnia, A ferroelectric quantum phase transition inside the superconducting dome of $\text{Sr}_{1-x}\text{Ca}_x\text{TiO}_{3-\delta}$, *Nat. Phys.* **13**(7), 643–648 (2017), <https://doi.org/10.1038/nphys4085>
- [18] S.E. Rowley, L.J. Spalek, R.P. Smith, M.P.M. Dean, M. Itoh, J.F. Scott, G.G. Lonzarich, and S.S. Saxena, Ferroelectric quantum criticality, *Nat. Phys.* **10**(5), 367–372 (2014), <https://doi.org/10.1038/nphys2924>
- [19] C.L. Wang and M.L. Zhao, Burns temperature and quantum temperature scale, *J. Adv. Dielectr.* **1**(2), 163–167 (2011), <https://doi.org/10.1142/S2010135X1100029X>
- [20] N. Barman, P. Singh, C. Narayana, and K. Varma, Incipient ferroelectric to a possible ferroelectric transition in Te^{4+} doped calcium copper titanate ($\text{CaCu}_3\text{Ti}_4\text{O}_{12}$) ceramics at low temperature as evidenced by Raman and dielectric spectroscopy, *AIP Adv.* **7**(3), 035105 (2017), <https://doi.org/10.1063/1.4973645>
- [21] M. Maior, M. Gurzan, S. Molnar, I. Prits, and Y. Vysochanskii, Effect of germanium doping on pyroelectric and piezoelectric properties of $\text{Sn}_2\text{P}_2\text{S}_6$ single crystal, *IEEE Trans. Ultrason. Ferroelectr. Freq. Control* **47**(4), 877–880 (2000), <https://doi.org/10.1038/nphys2924>
- [22] V.S. Vikhnin, P.A. Markovin, and W. Kleemann, The origin of polar ordering in incipient ferroelectrics with weak off-center impurities, *Ferroelectrics* **218**(1), 85–91 (1998), <https://doi.org/10.1080/00150199808227136>
- [23] P. Barone, D. Di Sante, and S. Picozzi, Improper origin of polar displacements at CaTiO_3 and CaMnO_3 twin walls, *Phys. Rev. B* **89**(14), 144104 (2014), <https://doi.org/10.1103/PhysRevB.89.144104>

KVANTINIS PARAELEKTRIŠKUMAS IR INDUKUOTASIS FEROELEKTRIŠKUMAS ĮTERPIANT GERMANIĄ Į $(\text{Pb}_y\text{Sn}_{1-y})_2\text{P}_2\text{S}(\text{Se})_6$ KRISTALUS

I. Zamaraitė^a, A. Džiaugys^a, Yu. Vysochanskii^b, J. Banyš^a

^a *Vilniaus universiteto Fizikos fakultetas, Vilnius, Lietuva*

^b *Užgorodo universiteto Kietojo kūno fizikos ir chemijos institutas, Užgorodas, Ukraina*

Santrauka

Darbe tyrinėjamos keturių kristalų – $\text{Pb}_2\text{P}_2\text{S}_6$, $(\text{Pb}_{0.98}\text{Ge}_{0.02})_2\text{P}_2\text{S}_6$, $(\text{Pb}_{0.7}\text{Sn}_{0.3})_2\text{P}_2\text{S}_6 + 5\% \text{Ge}$ ir $(\text{Pb}_{0.7}\text{Sn}_{0.3})_2\text{P}_2\text{Se}_6 + 5\% \text{Ge}$ – dielektrinės savybės intervale nuo kambario temperatūros iki 20 K. Atlikti tyrimai leido nustatyti kvantinę paraelektrinę būseną kristaluose, kuriuose buvo įterpta germanio priemaišų.

Visose tirtose medžiagose stebėtas atvirkštinės dielektrinės skvarbos nukrypimas nuo Kiuri ir Veiso dėsnio, aprašytas T^2 temperatūrine priklausomybe. Tirtųjų kristalų dielektrinės skvarbos temperatūrinės priklausomybės analizuotos remiantis Barrett'o modeliu.